Research Article

Surface oxidized and un-oxidized activated carbon derived from *Ziziphus jujube* Stem, and its application in removal of Cd(II) and Pb(II) from aqueous media

Nadir Khan[1] · Fazal Wahid[1] · Qamar Sultana[2] · Najm Us Saqib[3] · Muhammad Rahim[3]

Abstract

Agricultural waste based low cost oxidized activated carbon (OSD) and un-oxidized activated carbon (USD) samples were prepared from saw dust of *Ziziphus jujube* by chemical activation with phosphoric acid (H_3PO_4). The activated carbon was used for the removal of toxic metal ions such as cadmium(II) and lead(II) from aqueous solutions. The effect of pH (2–9), initial concentration (70–100 mg/L), contact time (5–700 min), activated carbon dose (0.1–1.0 g) and temperature (298–328 K) was investigated. In addition, the kinetic study was performed at pH 6, while the carbon dose of 0.1 g was used for 40 mL solution of 70 mg/L at four different temperatures (298, 308, 318 and 328 K). The adsorption efficiency of USD was found higher than OSD. Comparatively higher uptake of Pb(II) ions was observed by each carbon sample. Pseudo-second order equation best fitted the experimental data. As such, both activated carbon samples (USD and OSD) exhibited higher adsorption capacities and faster kinetics which revealed their commercial usefulness.

Keywords Activated carbon · Adsorption · Kinetics · Cadmium · Lead · *Ziziphus jujube*

1 Introduction

Heavy metals are potential water pollutants [1] due to their toxic and non-biodegradable nature that pose a severe threat to public health and the environment [2, 3]. The main sources of metal pollution are tannery, mining [4], metallurgy, electroplating, production of chemicals, painting, battery production, surface modification industry, garbage incinerator, sludge discharge, processing of radioactive materials, production of electric equipment, pesticides and fertilizers [5] and dyes [6]. According to the World Health Organization (WHO), aluminum, chrome, cobalt, nickel, copper, cadmium, zinc, mercury, and lead are considered as toxic metals [7, 8]. The adverse effects of heavy metal ions on humans [9] and other living organisms are continuously increasing from the last of few decades [10, 11]. The WHO reported that about 50,000 people die each day as a result of water pollution [12]. Cadmium (Cd) and lead (Pb) are the heavy metals which are most likely to be found in waste water [13, 14] that may ultimately find their way into the natural water resources [15–17]. Cadmium is a non-essential toxic heavy metal which is commonly used in batteries, pigments, corrosion resistant coatings [18], ceramics and textile printing [19]. It is generally released into the environment as a result of burning of fossil fuels, use of phosphate fertilizers, incineration of municipal solid wastes, tobacco smoking, and manufacturing of iron, steel and cement [20]. Similarly, lead is highly toxic metal that adversely affects the living organisms [21]. It is used in construction material, corrosion resistant, electrode material, shield for radiation and automobile batteries. Lead may enter the water bodies through effluents from paints, pigments, batteries, solders, alloying

✉ Muhammad Rahim, kpk566@gmail.com | [1]Department of Chemistry, Government College Peshawar, Khyber Pakhtunkhwa, Pakistan. [2]National Center of Excellence in Physical Chemistry, University of Peshawar, Khyber Pakhtunkhwa, Pakistan. [3]School of Chemical Sciences, Universiti Sains Malaysia, 11800 Pulau, Penang, Malaysia.

and mining activities [22]. It may enter to the environment by combustion of leaded gasoline in the internal combustion engines [23, 24]. According to World Health Organization (WHO), the permissible limits of cadmium and lead in drinking water are 0.003 mg/L and 0.001 mg/L, respectively [25].

Several studies have revealed that cadmium and lead concentrations in drinking water in Pakistan particularly in urban areas are above the maximum permissible limits of W.H.O.[25]. Due to the toxic nature of cadmium and lead, their removal from potable and waste waters by eco-friendly methods is of utmost importance [26]. Most of the methods used for water treatment are expensive, technically complicated or associated with toxic wastes disposal problems. Adsorption is an effective, simple, environment friendly and cost effective method for the uptake of heavy metal ions from aqueous media [27, 28]. The use of agricultural wastes for preparation of activated carbons is increasing due to their better adsorption capacities and cost effectiveness. Various agricultural wastes like corn cobs, hazelnut shells, date stones and nutshells have been used by researchers for the preparation of activated carbons. Whereas, the agro-carbons of varying surface area, pore volumes and pore size distribution can be prepared by controlling the conditions of carbonization process [29, 30].

The present study focuses on the preparation of surface oxidized and un-oxidized activated carbon from saw dust of *Ziziphus jujube* (Ber) plants by chemical activation with phosphoric acid (H_3PO_4). A very little work has been reported in literature regarding the use of *Ziziphus jujube* as starting material for preparation of activated carbon. Pandharipade et al. (2012) has reported synthesis of adsorbents from waste materials of the *Ziziphus jujube* seed [31]. As such, a large volume of *Ziziphus jujube* saw dust is produced by saw mills in Pakistan which is of no specific utilization as useful commodity. The saw dust is discharged and dispersed into the environment without proper disposal management that may cause several potential hazards. The conversion of such agricultural wastes into valuable products like activated carbons for the removal of toxic metal ions from aqueous solutions is of great importance from both environmental and economic point of view. The prepared carbon samples were utilized for the adsorptive removal of Cd(II) and Pb(II) metal ions from aqueous solutions.

2 Materials and methods

2.1 Chemicals and instruments

Analytical grade chemicals, H_3PO_4 (CAS: 7664–38-2), HCl (No. 109,058), NaOH (CAS: 1310–73-2), $Cd(NO_3)_2$ (No.

102,019) and $Pb(NO_3)_2$ (CAS: 10099–74-8) were purchazed from Merck, Germany. Water was freshly distilled prior to use.

The pH was measured with pH meter (model 744, Metrohm) equipped with a combined glass-saturated calomel electrode calibrated with buffer solutions of pH ~ 4.0, pH ~ 7.0 and pH ~ 10.0. The nitrogen adsorption isotherms were determined with a Quantachrome NOVA 2200e, surface area and pore size analyzer. The carbon samples were dried in program controller Nebertherm C-19 (model N 7/4 W—Germany). Metal ion concentration was determined using atomic adsorption spectrophotometer (Shimadzu model AA670). The carbonization was carried out in a muffle furnace (model No TF 55030C-1 Thermo electron Corporation, USA) and washing was carried out in a Soxhlet extractor.

2.2 Preparation of activated carbon

Activated carbon was prepared from saw dust of *Ziziphus jujube*. The saw dust was washed with distilled water and dried at 110 °C for 24 h. The sample was mixed with 50% aqueous solution of H_3PO_4 (weight ratio; 1:1). The mixture was allowed to soak for 24 h at room temperature. The sample was heated in a horizontal tube furnace at 170 °C for one hour under nitrogen atmosphere with flow rate of 100 mL per minute then the temperature was increased to 450 °C for one hour under the same flow rate of nitrogen. The carbonized sample was cooled to room temperature in an inert atmosphere of nitrogen, and the sample was named, un-oxidized activated carbon (USD). Half of the USD sample was oxidized by using breathing grade air at a flow rate of 100 mL per minute at 450 °C for one hour and cooled in the breathing grade air to room temperature. The sample was named, oxidized activated carbon (OSD). Both the activated carbon samples were rinsed with double distilled water in Soxhlet extractor at 100 °C until the pH of the rinsing water become neutral. The samples were dried at 110 °C for 24 h and cooled in desiccators. The cooled samples were sieved and the desired particle size of 170–400 mesh was obtained [32].

2.3 Characterization of activated carbon

The prepared activated carbon samples were characterized by determination of pH, PZC, surface area, pore volumes and surface functional groups. BET surface area and pore structure were determined by nitrogen adsorption method at 77 K using Quantachrome NOVA 2200e, surface area and pore size analyzer. The micro-pore and total pore volume was determined by BJH method. The mesopore volume was calculated by subtracting the micro-pore volume from the total pore volume. The acidic and basic

surface functional groups of each sample were quantified by Boehm's titration method [33].

2.4 Adsorption studies

Batch experiments were performed at different pH (2–9), initial concentrations (70–100 mg/L), temperatures (298–328 K), activated carbon dosages (0.1–1.0 g) and contact time (5–700 min). Kinetic study was performed using initial concentration of 70 mg/L and pH ~6 at different temperatures (298, 308, 318 and 328 K). In batch experiment, 0.1 g of either USD or OSD was added to 40 mL solution of the desired concentration. The initial pH of the solution was adjusted using 0.10 M HCl / NaOH solution. The solution was shaken at a speed of 110 rpm. After shaking, the final pH of solution was recorded and filtered discarding the first 5 mL fraction of each filtrate. The filtrate was analyzed for residual metal ions concentration by using atomic adsorption spectrophotometer. During contact time and kinetic study, each solution was agitated for predetermined time intervals and filtered. The amount of each metal ion adsorbed (q_e) was calculated by the Eq. 1.

$$q_e = \frac{(C_i - C_e)V}{W \times 1000} \qquad (1)$$

where C_i and C_e are the initial and equilibrium concentrations (mg/L) of metal ions in solution, V is the volume (L) and W is the amount of adsorbent in grams.

3 Results and discussion

3.1 Characterization

Characteristics of the un-oxidized activated carbon (USD) and oxidized activated carbon (OSD) are listed in Table 1. It is evident from the table that both the activated carbon samples have greater pore volumes along with micropores and meso-pores. Above 90% of the total pore volume of each sample comprised of micro-pores. The higher BET and lower BJH surface areas also suggested the microporous nature of the carbon samples. The increased BET surface area and pore-volumes could be attributed to strong chemical interaction and diffusion of the activating agent (H_3PO_4) into the inner structure of the precursor material during soaking and impregnation [34]. The activating agent becomes evaporated along with other volatile matter during carbonization [35, 36]. Table 1 shows that pH and PZC of aqueous solution of both samples were in acidic range that might be due to the presence of acidic functional groups dominantly lactonic, phenolic and carboxylic functional groups

Table 1 Characteristic parameters of the OSD and USD activated carbon samples

S. no	Properties	USD*	OSD**
1	pH	4.83	4.46
2	PZC	4.90	4.52
3	Apparent density (g mL^{-1})	1.26	2.52
4	Bulk/Tap density (g mL^{-1})	1.13	2.16
5	Surface area (SBET), m^2/g	443	602
6	Surface area (SBJH), m^2/g	23.3	29.7
7	Micro-pore volume (cc/g)	0.23	0.31
8	Total pore volume (cc g^{-1})	0.24	0.34
9	Meso-pore volume (cc g^{-1})	0.02	0.03
10	Average pore radius*** (A°)	11.2	11.2
11	Adsorption energy (KJ/mol)	10.4	10.2
12	% Carbon content	67.4	59.7
13	% Oxygen content	22.1	28.9
14	% Phosphorus content	4.14	5.28
15	%Ash content	1.67	1.89
16	Carbonyl (m mol g^{-1})	0.00	0.00
17	Phenolics + lactonics × 10^{-3} (m mol g^{-1})	2.32	1.56
18	Carboxylics × 10^{-3} (m mol g^{-1})	1.80	1.83
19	Quinone × 10^{-3} (m mol g^{-1})	3.97	4.14
20	Basic groups × 10^{-3} (m mol g^{-1})	1.04	0.87

*Surface Un-Oxidized Activated Carbon

**Surface Oxidized Activated Carbon

*** Average pore radius = 2(VTotal) / SBET

on their surfaces. The acidic functional groups are likely to be introduced during interaction and destruction of the pore walls of carbon samples by phosphoric acid, resulting in deposition of large number of oxygen containing acidic functional groups. The more acidic surface, higher S_{BET}, S_{BJH}, micro-pore volume, average pore-radius and pore volume of the oxidized sample as compared to un-oxidized sample could be explained in terms of air oxidation. The air oxidation might have introduced more oxygen containing acidic functional groups and facilitated the evolution of volatile matter from the precursor materials during carbonization [29, 37].

3.2 Adsorption studies

3.2.1 Effect of contact time and initial concentration

Contact time study helps to determine the rate of adsorption and equilibrium time. The uptake rate is an important aspect; higher adsorption rate indicates higher affinity of adsorbent towards metal ions, and to reach equilibrium state earlier. Equilibrium time depends on the nature, compactness and other textural properties of the adsorbent. Results of the effect of contact time on the adsorption

process are shown in Fig. 1. The results clearly illustrate that the adsorption of both the metal ions increased with the contact time until equilibrium was established. The USD indicated the equilibrium time of 480 min for both cadmium and lead while the OSD showed the equilibrium time of 420 min for both metal ions. The adsorption of the metal ions was very fast in the beginning which then becomes slow and finally constant after equilibrium. The higher adsorption in the early stages might be due to the larger number of available sites on the adsorbent surface. The subsequent slower adsorption is likely due to the competition among the metal ions for the limited number of unsaturated adsorption sites. When the adsorbent surface becomes saturated, the diffusion of the metal ions into the bulk of the adsorbent becomes slower and the adsorption rate decreases.

Furthermore, the results indicate that the sorption capacity of the adsorbent increased with the increase of initial concentration, as shown in Fig. 1. This could be attributed to the increased driving force that minimizes the resistance to mass transfer of metal ions in solution towards the adsorbent surface. At lower concentrations, the number of metal ions available in the solution is less as compared to the sufficiently available active sites on the adsorbent surface, hence rate of adsorption is higher but the amount adsorbed per unit mass of adsorbent is lesser.
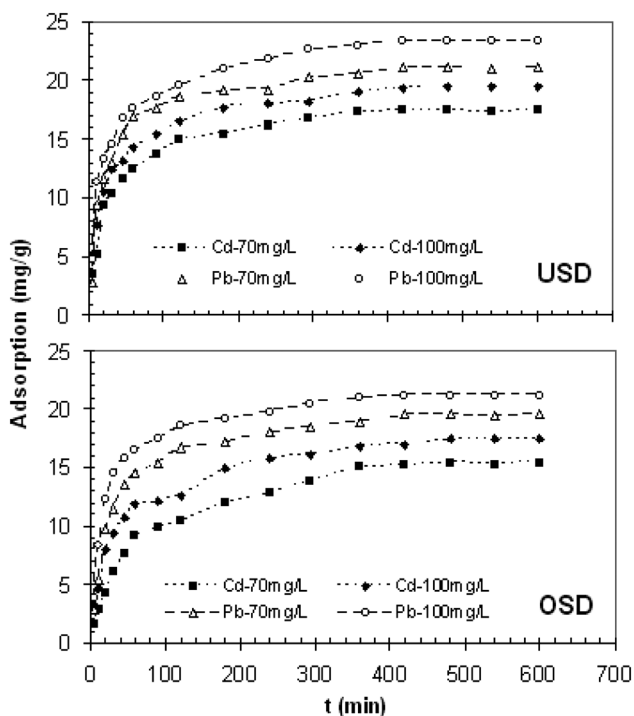
The increased adsorption of metal ions from solution of higher initial concentrations might be due to covering of all the active sites of adsorbent surface by the sufficient number of metal ions available in the solution.

3.2.2 Effect of pH

pH of the solution is one of the most important parameters, which strongly influences the removal of metal ions from their aqueous solution. It affects the surface charge of adsorbent as well as the solubility and ionic state of metal ion. Activated carbon is amphoteric in nature and at lower pH below pH_{PZC}, its surface becomes positively charged due to high protonation while at higher pH above pH_{PZC}, its surface bears negative charge due to higher concentration of OH^{-1} ions than H^{+1} ions. As a result of increased electrostatic attraction, higher adsorption of metal anions occurs at lower pH while favorable adsorption of metal cations takes place at higher pH [38].

The effect of pH on adsorption of Cd(II) and Pb(II) ions was studied in the pH range of 2–9 as illustrated in Fig. 2. As expected the adsorption of both the metal ions increased with increase in initial pH of the solution. The lower adsorption at lower pH could be explained in terms of repulsion between metal cations and positively charged surface of activated carbon. The increased adsorption at higher pH might be due to increased electrostatic attraction between metal cations and negatively charged surface of activated carbon. Indeed the final pH of solution after each metal ions adsorption was found lower than the initial pH which indicated the release of H^{+1} from the adsorbent surface. The decrease in final pH also suggested that the adsorption of Cd(II) and Pb(II) ions involved an ion-exchange mechanism. As such, OSD indicated lower
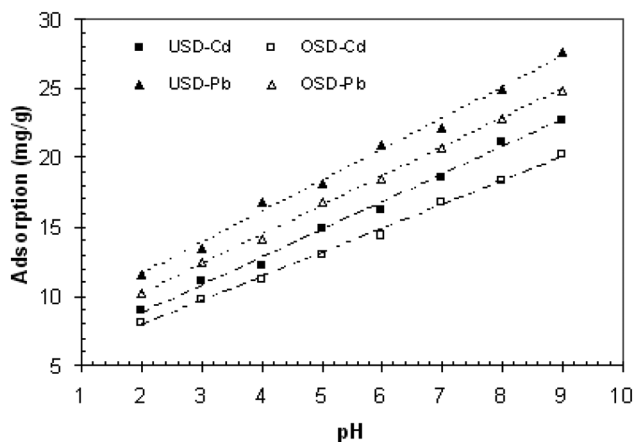

Fig. 1 Effect of contact time and initial concentration on Cd(II) and Pb(II) adsorption (pH 6; T = 298 K; Carbon Dose = 0.1 g, Shaking Speed = 110 rpm)

Fig. 2 Effect of pH on Cd(II) and Pb(II) adsorption (Initial Conc: = 70 mg/L; T = 298 K; Carbon Dose = 0.1 g; Shaking Speed = 110 rpm)

uptake of metal ions as compared to USD. This might be explained in terms of more acidic surfaces of oxidized samples due to the presence of oxygen containing acidic groups. Higher adsorption of Pb(II) ions occurred than Cd(II) ions under the same conditions, most likely due to smaller size of Pb(II) ions. Most of the metals precipitate at higher pHs, hence to avoid any precipitation of metal ions and being closer to pH of natural water, pH 6 was selected as the optimum pH for the adsorption of Cd(II) and Pb(II) ions from aqueous solutions and all the batch experiments were performed at pH ~ 6.

3.2.3 Effect of temperature

The adsorption of metal ions from aqueous solution is highly temperature dependent. Temperature affects the adsorption capacity of porous adsorbent by changing the number of active sites and/or chemical interaction between metal ions and the adsorbent surface. Therefore, the effect of temperature was evaluated at four different temperatures (298, 308, 318 and 328 K) at pH ~ 6 and initial concentration of 70 mg/L.

The results showed that the adsorption of Cd(II) and Pb(II) ions increased with the increase in temperature, as shown in Fig. 3. The enhanced removal at higher temperatures indicated the endothermic nature of adsorption process. The temperature rise might be resulted in creation of some new active sites on adsorbent surface or enhanced interaction between metal ions and adsorbent, leading to increased adsorption. Additionally an increase in temperature decreases the viscosity of the solution due to which the metal ions become more mobile leading to increased diffusion through an external boundary layer and into the pores of the adsorbent surface. At each temperature, USD sample exhibited higher adsorption capacity for both the metal ions.

3.2.4 Effect of carbon dosage

The effect of carbon dosage on removal of Cd(II) and Pb(II) ions was studied in a batch system using carbon dose of 0.1– 1.0 g. Whereas, the initial metal ion concentration, pH and temperature was chose as 70 mg/L, 6 and 298 K, respectively. The results illustrated that the adsorption of Cd(II) ions decreased from 16.47–3.08 mg/g and 14.35–2.36 mg/g while that of Pb(II) ions decreased from 20.98–5.28 mg/g and 18.56–4.19 mg/g respectively by USD and OSD samples when carbon dosage increased from 0.1 to 1.0 g. The decrease in the amounts of Cd(II) and Pb(II) ions adsorbed by both the activated carbon samples might be due to aggregation of adsorbent particles because of the presence of larger number of metal ions in the solution which results in decreasing the active surface.
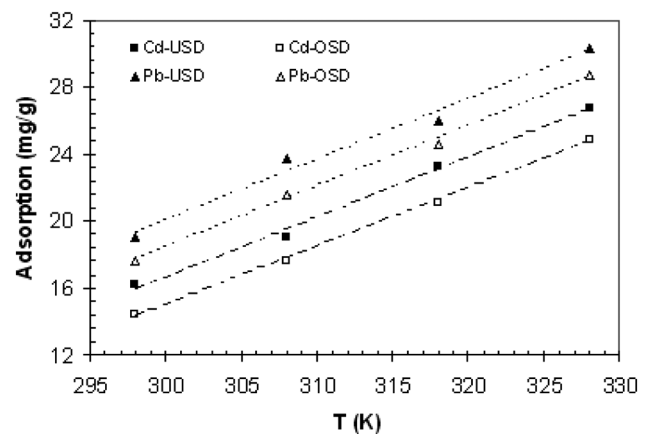

Fig. 3 Effect of temperature on Cd(II) and Pb(II) adsorption (pH 6; Initial Conc = 70 mg/g; Carbon Dose = 0.1 g; Shaking Speed = 110 rpm)

The active sites of the clustered adsorbent particles are not accessible by the metal ions, resulting in the decreased adsorption capacity [39, 40].

The literature survey indicate that the maximum adsorption capacity of different materials towards Cd^{2+} and Pb^{2+} are 7.28 and 7.39 [41], 80.64 and 93.45 mg/g [13], 29.23 and 31.44 [42], 92.4 and 94.5 mg/g [43] respectively, for cadmium and lead. Cadmium showed maximum adsorption capacities of 9–10 [44], 72.62 [45], 88.75 [46] 31.65 [47], 81.02 [48], 45.58 [49] and 21.6 mg/g [50]. Whereas, lead indicated maximum adsorption capacities of 97.5 [51], 417 [52], 263.6 [53] and 328.9 mg/g [54]. The literature values are summarized in Table 2.

3.3 Kinetics studies

3.3.1 Pseudo-first order equation

The pseudo first-order and pseudo second-order kinetic models were applied to analyze the experimental data and results are summarized in Table 3. Pseudo first-order equation is shown in Eq. 2.

$$\log \left(\frac{qe}{qe - qt} \right) = \frac{k_1}{2.303} t \tag{2}$$

where q_t and qe are the amounts of metal ions adsorbed (mg/g) at time t and equilibrium time, respectively. k_1 (min^{-1}) is the rate constant of pseudo first order kinetic equation. The values of k_1 and qe are calculated from the intercepts and slopes of the linear plots of log (qe-qt) versus t. Table 3 shows that the predicted values of linear regression correlation coefficient (R^2) of pseudo first-order for both Cd(II) and Pb(II) ions adsorption at all temperatures are almost ≥ 0.90. However, the difference

Table 2 Literature comparison of the maximum adsorption capacities

S. No	Type of material	Cd^{2+} (mg/g)	Pb^{2+} (mg/g)
01	*Rhizopus oryzae* biomass	7.28	7.39
02	*Padinasanctae crucis* biomass	93.45	80.64
03	*Callinectes sapidus* biomass	29.23	31.44
04	*Phoenix dactylifera* activated carbon	94.5	92.4
05	Activated carbon	9 to 10	–
06	Titanium-modified ultrasonic biochar	72.62	–
07	Alkaline silicate wastes	88.75	–
08	Raw and Acid Activated Wheat Straw Biochar	31.65	–
09	Surface-Modified Biochar	81.02	–
10	Corncob-supported aluminium-manganese binary oxide composite	45.58	–
11	Microalgae-endophyte symbiotic system	21.6	–
12	Iron oxide nanomaterials	–	97.5
13	Magnetic silica-based hybrid organic–inorganic nanocomposite	–	417
14	CeO_2–MoS_2 hybrid magnetic biochar	–	263.6
15	Two-dimensional MAX-derived titanate nanostructures	–	328.9

between the theoretical and experimental adsorption capacities suggests that the kinetic data can not be interpreted by pseudo first order model. Similar results are also observed by other researchers for adsorption of metal ions from aqueous solutions using activated carbon [32, 55]. Therefore, pseudo second-order equation was applied. The pseudo second-order rate equation is shown in Eq. 3.

$$\frac{t}{q_t} = \frac{1}{k_{2ads}q_e^2} + \frac{t}{q_e} \qquad (3)$$

where q_t and q_e are the amounts of metal ions adsorbed (mg/g) at time t and equilibrium time (mg/g), respectively. k_2 (g mg^{-1} min^{-1}) is the rate constant of pseudo second-order kinetic equation. The pseudo second order rate constant (k_2) and the equilibrium adsorption capacity (q_e) are calculated from the intercepts and slopes of the linear plots of *log* (t/q_t) versus *t*. The linear plots of *log* (t/q_t) versus *t* are shown in Fig. 4. The linearity of plots suggests that pseudo second order rate equation is applicable to describe the experimental data. In addition, Table 3 shows that R^2 values ≥ 0.99. As such, the calculated adsorption capacity (q_e) is in close agreement to the experimental values, indicating that the pseudo second order rate equation is better fitted to describe the adsorption kinetic data. Fitting of the pseudo second order rate equation also supports the chemical nature of metal ions adsorption by the USD and OSD samples [42, 43, 56].

3.4 Mechanism of adsorption kinetics

3.4.1 Weber and Morris model

Weber and Morris model is applied to investigate the intra-particle diffusion as the rate limiting step. According to Weber and Morris [57], the intra-particle diffusion model is expressed in Eq. 4.

$$qt = K \times t^{1/2} + C \qquad (4)$$

where qt (mg g^{-1}) is amount of metal ions adsorbed at time *t*, K (mg^{-1} g min$^{-1/2}$) is the intra-particle diffusion rate constant and C (mg g^{-1}) is related to the thickness of the boundary layer. The value of C depicts resistance to mass transfer in the boundary layer, larger the value of C, greater is the boundary layer effect and vice versa. The values of K and C calculated from the slope and intercept of the plots of qt against $t^{1/2}$, as listed in Table 3. Linear plots of qt versus $t^{1/2}$ for Cd(II) and Pb(II) ions adsorption by the prepared carbon samples are shown in Fig. 5. The linearity of plots indicates that adsorption process involves intra-particle diffusion. However, intra-particle diffusion is the rate controlling step if the straight lines pass through the origin with no intercepts. When plots show multi-linearity, then the adsorption process may involve more than one step. Although the intra-particle diffusion model plots are

Fig. 4 Pseudo-second order model plots for Cd(II) and Pb(II) adsorption (pH 6; Initial Conc = 70 mg/g; Carbon Dose = 0.1 g; Shaking Speed = 110 rpm)
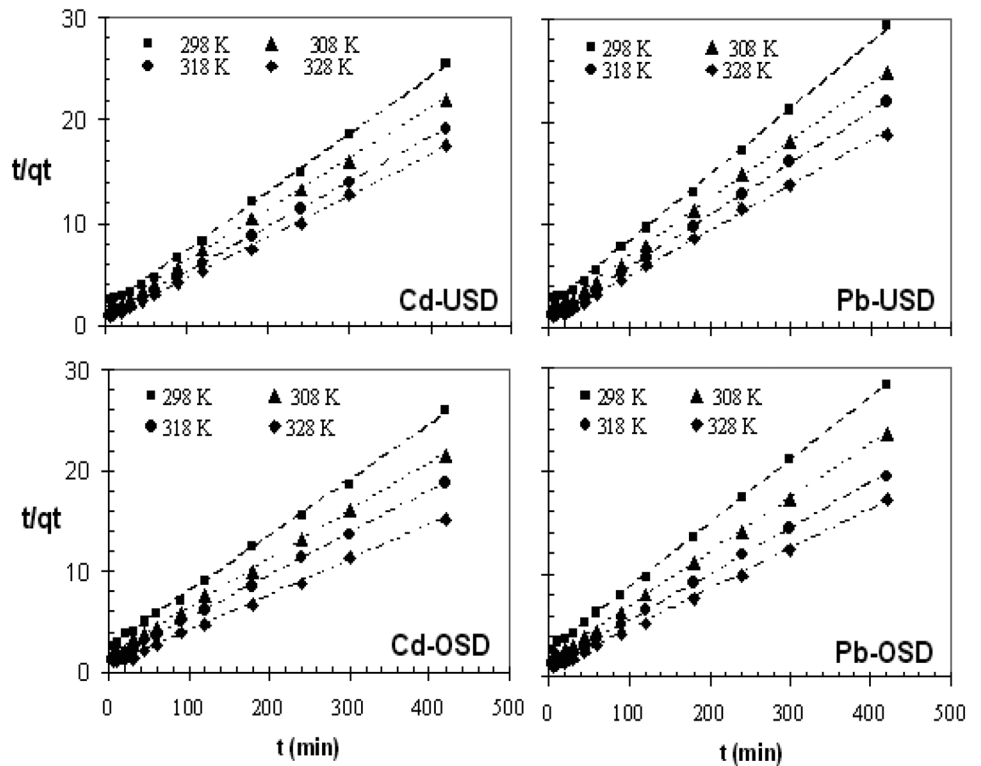

Table 3 Constant values of pseudo first and pseudo second-order equations

Pseudo first order kinetic constants								Pseudo second order kinetic constants					
Sample	T (K)	Cadmium(II)			Lead(II)			Cadmium(II)			Lead(II)		
		R^2	$K_1 \times 10^{-3}$	q_1	R^2	$K_1 \times 10^{-3}$	q_1	R^2	$K_2 \times 10^{-4}$	q_2	R^2	$K_2 \times 10^{-4}$	q_2
USD*	298	0.961	20.72	14.52	0.980	8.981	11.99	0.999	02.17	17.39	0.998	1.324	17.73
	308	0.968	14.74	11.74	0.974	10.59	12.81	0.999	02.52	19.53	0.999	1.689	20.12
	318	0.955	15.20	10.28	0.969	12.21	13.58	0.999	03.07	21.74	0.999	1.790	22.83
	328	0.960	1472	12.89	0.970	17.27	16.69	0.999	02.52	25.13	0.999	2.054	26.52
OSD**	298	0.896	09.67	06.63	0.909	11.75	10.03	0.999	03.57	13.75	0.997	2.138	14.99
	308	0.915	10.82	08.63	0.907	9.673	9.328	0.999	02.66	17.76	0.999	2.359	17.67
	318	0.891	10.36	10.08	0.921	11.05	10.92	0.999	02.42	20.92	0.999	2.142	21.50
	328	0.901	09.21	11.35	0.912	9.212	12.29	0.999	02.12	24.45	0.998	1.975	24.94

*Surface un-oxidized activated carbon

**Surface oxidized activated carbon

straight lines but the straight lines do not pass through the origin. The values of the correlations coefficients R^2 are also lower than 0.90. As a whole the results indicate that the intra-particle diffusion is involved but not the only rate controlling step for the adsorption of Cd(II) and Pb(II) ions onto both the activated carbon samples. The increase in the values of intra-particle diffusion rate constant (K) with increase in temperature is probably due to the increased diffusion of the metal ions into the pores of the adsorbent. It may be caused by the decrease in the viscosity

of the solution with increase in temperature that leads to increased adsorption.

3.4.2 Boyd model

The experimental data was not fitted in Langmuir and Freundlich isotherm models therefore, Boyd model is used to differentiate between film and intra-particle diffusion. The Boyd model is shown in Eq. 5.

Fig. 5 Weber and Morris model plots for Cd(II) and Pb(II) adsorption (pH 6; Initial Conc = 70 mg/L; Carbon dose = 0.1 g; Shaking speed = 110 rpm)
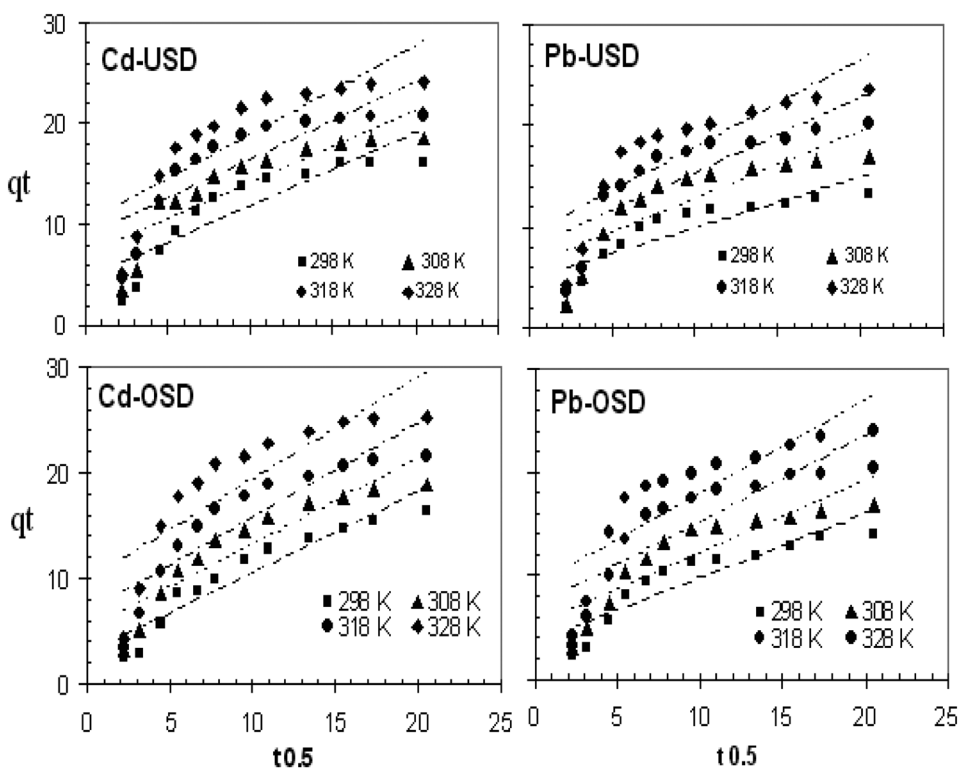
$$F = 1 - \frac{6}{\pi^2} \exp(-Bt) \qquad (5)$$

where F represents the fraction of solute adsorbed at any time t ($F = q_t/q_e$), and Bt is a mathematical function of F. Rearranging the above equation, we get [$Bt = -0.4977 - Ln(1 - F)$]. The Bt values are plotted versus time t at different temperatures. When the plots are linear, passing through the origin, then the rate controlling step is pore diffusion. When the plots are non linear or linear but not passing through the origin and have intercepts, then film diffusion is the rate controlling step.

The results of Boyd model are shown in Fig. 6. It can be seen from the results that the plots of Bt versus time t are linear but not passing through the origin, which indicate that the film diffusion process is the main controlling step. Kapur and Mondal have reported similar results for the adsorption of metal ions [58].

3.4.3 Estimation of activation energy

The Arrhenius equation gives important information about the activation energy (Ea). The linearized form of Arrhenius equation can be used to calculate the activation energy of adsorption which is shown in Eq. 6.

$$\ln k_2 = \ln A - \frac{E_a}{RT} \qquad (6)$$

where E_a is the activation energy, R is gas constant, k_2 is the rate constant obtained from pseudo second order plots, A is the pre-exponential factor and T is the solution temperature. Activation energy (E_a) values are calculated from the slopes of the plots of $ln\, k_2$ versus $1/T$. The values of activation energy in the range of 8.4–83.7 kJ mol^{-1}, indicated chemical type of adsorption. Activation energy also gives concept of the rate-limiting step of the adsorption process. An adsorption process is diffusion controlled when $E_a < 42$ kJ mol^{-1} while adsorption process is considered to be chemically controlled when $E_a > 42$ kJ mol^{-1}. The values of activation energy for adsorption of Cd(II) and Pb(II) ions from aqueous solutions by USD and OSD sample are listed in Table 3. Table 3 shows that the values of activation energy for Cd(II) ions adsorption by USD and OSD sample were 11.81 kJ mol^{-1} and 12.59 kJ mol^{-1} respectively while for Pb(II) adsorption were found to be 10.49 kJ mol^{-1} and 11.57 kJ mol^{-1} respectively. The calculated values of activation energy were found within the range of 8.4–83.7 kJ mol^{-1} indicating chemisorptions. Moreover, the values of activation energy are lower than 42 kJ mol^{-1}, suggested that the rate limiting step is to be diffusion controlled. The metal ions from bulk solution to the adsorption sites of activated carbon surface may be transported through surface diffusion, bulk diffusion or pore diffusion. These processes are in series rather than parallel and the slowest one is the rate-controlling step

Fig. 6 Boyd model plots for Cd(II) and Pb(II) adsorption (pH 6; Initial Conc = 70 mg/L; Carbon dose = 0.1 g; Shaking speed = 110 rpm)
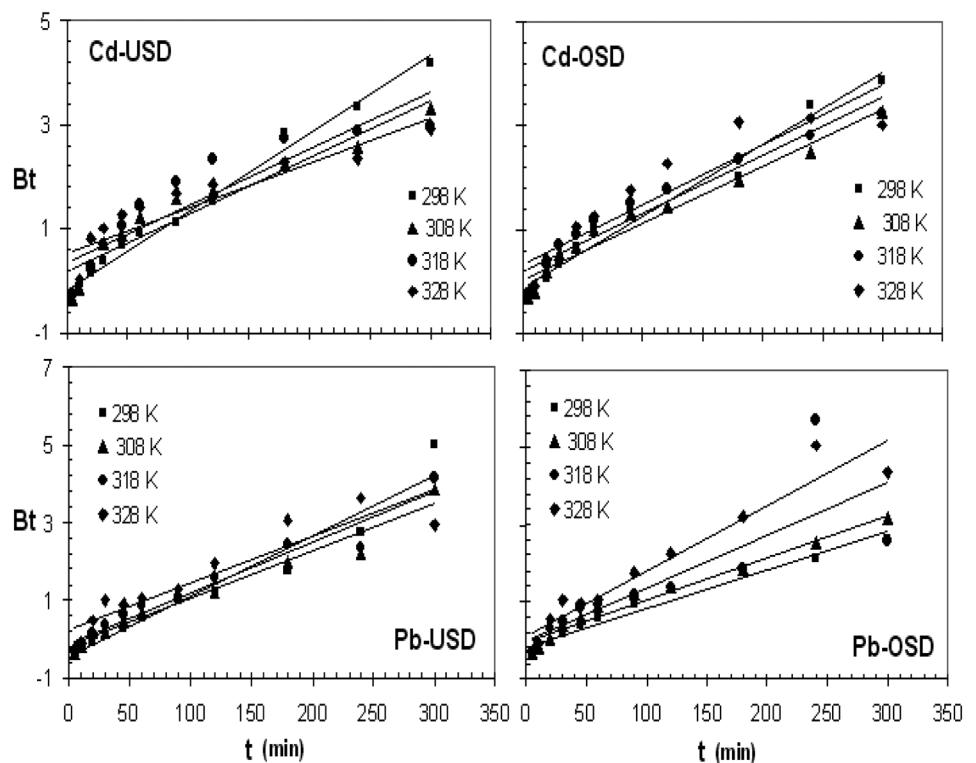
which in turn determines the overall kinetics of adsorption [59].

3.5 Desorption studies

Desorption studies were performed using HCl solution which has been reported to be an efficient metal desorbing agent [60, 61]. After adsorption of Cd(II) and Pb(II) ions from their aqueous solutions of initial concentration 70 mg/L at 298 K and pH 6, each carbon sample loaded with metal ions was separated by centrifugation. The carbon was washed gently with triply distilled water to remove any un-adsorbed metal ions. The spent carbon was agitated with 70 mL of 0.1 M HCl solution for 5 h and the concentration of desorbed metal ions was determined by using atomic absorption spectrophotometer. The regeneration efficiency was investigated upto three consecutive adsorption–desorption cycles. After three cycles, the adsorption capacity of USD and OSD sample decreased from 89.83 to 67.46% and 82 to 54.6% for Cd(II) ions and 91.47% to 74.32% and 86.5 to 60.87% for Pb(II) ions respectively.

4 Conclusion

The surface oxidized (OSD) and un-oxidized activated carbon (USD) samples were derived from saw dust of the *Ziziphus jujube* plant by chemical activation process. The

samples indicated higher BET surface area, greater pore size distribution and more surface functional groups. Based on the above properties and cost effectiveness, the OSD and USD samples were used for the successful adsorption of Cd(II) and Pb(II) metal ions from aqueous solutions. The effect of initial concentration, pH, adsorbent dose and temperature was evaluated. The uptake of metal ions increased with increase in initial pH, concentration and temperature. The adsorption capacity of un-oxidized sample was found higher than surface oxidized activated sample. As such, OSD and USD samples indicated higher uptake of Pb(II) as compared to Cd(II). In addition, both OSD and USD exhibited excellent adsorption capacities and faster adsorption rates. Pseudo second-order equation better fitted the adsorption data. Desorption study showed sufficient ease of regeneration. The overall results indicated that the prepared saw dust activated carbon samples could be used as low cost and environment friendly adsorbent for the effective removal of toxic metals ions such as Cd(II) and Pb(II) from aqueous solutions. The *Ziziphus jujube* activated carbon is strongly recommended for the removal of Cd(II) and Pb(II) from the industrial wastewater.

Our research group is working on the adsorption of other heavy metal ions from aqueous media using *Ziziphus jujube* OSD and USD samples.

Compliance with ethical standards

Conflict of interest The authors declare that there is no conflict of interest.

References

1. Abshirini Y, Foroutan R, Esmaeili H (2019) Cr(VI) removal from aqueous solution using activated carbon prepared from *Ziziphus spina*–christi leaf. Mater Res Express 6(4):045607

2. Javed M, Ahmad MI, Usmani N, Ahmad M (2017) Multiple biomarker responses (serum biochemistry, oxidative stress, genotoxicity and histopathology) in *Channa punctatus* exposed to heavy metal loaded waste water. Sci Rep 7(1):1–11

3. Rahim M, Ullah I, Khan A, Haris MRHM (2016) Health risk from heavy metals via consumption of food crops in the vicinity of District Shangla. J Chem Soc Pak 38(1):165–169

4. Foroutan R, Mohammadi R, Adeleye AS, Farjadfard S, Esvandi Z, Arfaeinia H, Sorial GA, Ramavandi B, Sahebi S (2019) Efficient arsenic (V) removal from contaminated water using natural clay and clay composite adsorbents. Environ Sci Pollut Res 26(29):29748–29762

5. Foroutan R, Mohammadi R, Farjadfard S, Esmaeili H, Ramavandi B, Sorial GA (2019) Eggshell nano-particle potential for methyl violet and mercury ion removal: surface study and field application. Adv Powder Technol 30(10):2188–2199

6. Foroutan R, Mohammadi R, Ramavandi B (2019) Elimination performance of methylene blue, methyl violet, and Nile blue from aqueous media using AC/CoFe 2 O 4 as a recyclable magnetic composite. Environ Sci Pollut Res 26(19):19523–19539

7. Shafiee M, Foroutan R, Fouladi K, Ahmadlouydarab M, Ramavandi B, Sahebi S (2019) Application of oak powder/Fe_3O_4 magnetic composite in toxic metals removal from aqueous solutions. Adv Powder Technol 30(3):544–554

8. Foroutan R, Oujifard A, Papari F, Esmaeili H (2019) Calcined Umbonium vestiarium snail shell as an efficient adsorbent for treatment of wastewater containing Co(II). 3Biotech 9(3):78

9. Foroutan R, Peighambardoust SJ, Mohammadi R, Omidvar M, Sorial GA, Ramavandi B (2020) Influence of chitosan and magnetic iron nanoparticles on chromium adsorption behavior of natural clay: adaptive neuro-fuzzy inference modeling. Int J Biol Macromol 151:355–365

10. Ahmad N, Rahim M, Haris M (2014) Toxicological impact assessment of heavy metals in human blood and milk samples collected in district Shangla. Pakistan Sci Int 26(1):223–226

11. Rahim M, Ullah I, Khan A, Haris MRHM, Ahmad N (2014) Spatial distribution and risk assessment of heavy metals from drinking water in District Shangla. Sci Int 26(4):1625–1630

12. Foroutan R, Zareipour R, Mohammadi R (2018) Fast adsorption of chromium (VI) ions from synthetic sewage using bentonite and bentonite/bio-coal composite: a comparative study. Mater Res Express 6(2):025508

13. Foroutan R, Esmaeili H, Sanati AM, Ahmadi M, Ramavandi B (2018) Adsorptive removal of Pb(II), Ni(II), and Cd(II) from aqueous media and leather wastewater using Padinasanctae-crucis biomass. Desalin Water Treat 135:236

14. Esvandi Z, Foroutan R, Mirjalili M, Sorial GA, Ramavandi B (2019) Physicochemical behavior of Penaeuse semisulcatuse chitin for Pb and Cd removal from aqueous environment. J Polym Environ 27(2):263–274

15. Rahim M, Mas Haris MRH (2015) Application of biopolymer composites in arsenic removal from aqueous medium: a review. J Radiat Res Appl Sci 8(2):255–263

16. Sastre J, Sahuquillo A, Vidal M, Rauret G (2002) Determination of Cd, Cu, Pb and Zn in environmental samples: microwave-assisted total digestion versus aqua regia and nitric acid extraction. Anal Chim Acta 462(1):59–72

17. Simoes MR, Ribeiro Junior RF, Vescovi MV, de Jesus HC, Padilha AS, Stefanon I, Vassallo DV, Salaices M, Fioresi M (2011) Acute lead exposure increases arterial pressure: role of the renin-angiotensin system. PLoS ONE 6(4):e18730

18. Thompson J, Bannigan J (2008) Cadmium: toxic effects on the reproductive system and the embryo. Reprod Toxicol 25(3):304–315

19. Nemmiche S, Chabane-Sari D, Kadri M, Guiraud P (2011) Cadmium chloride-induced oxidative stress and DNA damage in the human Jurkat T cell line is not linked to intracellular trace elements depletion. Toxicol In Vitro 25(1):191–198

20. Engstrom A, Skerving S, Lidfeldt J, Burgaz A, Lundh T, Samsioe G, Vahter M, Akesson A (2009) Cadmium-induced bone effect is not mediated via low serum 1,25-dihydroxy vitamin D. Environ Res 109(2):188–192

21. Rahman A, Brew BJ, Guillemin GJ (2011) Lead dysregulates serine/threonine protein phosphatases in human neurons. Neurochem Res 36(2):195–204

22. Popko J, Olszewski S, Hukałowicz K, Markiewicz R, Borawska M, Szeparowicz P (2003) Lead, cadmium, copper and zinc concentrations in blood and hair of mothers of children with locomotor system malformations. Pol J Environ Stud 12(3):375–379

23. Tripathi RM, Raghunath R, Vinod Kumar A, Sastry VN, Sadasivan S (2001) Atmospheric and children's blood lead as indicators of vehicular traffic and other emission sources in Mumbai, India. Sci Total Environ 267(1–3):101–108

24. Ahmad N, Khan LALI, Sattar A (2011) Potentiometric stripping analysis of heavy-metals in gasoline and dust particulate. J Chem Soc Pak 13(2):74

25. Azizullah A, Khattak MNK, Richter P, Häder D-P (2011) Water pollution in Pakistan and its impact on public health—a review. Environ Int 37(2):479–497

26. Rahim M, Mas Haris MRH (2019) Chromium (VI) removal from neutral aqueous media using banana trunk fibers (BTF)-reinforced chitosan-based film, in comparison with BTF, chitosan, chitin and activated carbon. SN Appl Sci 1(10):1180

27. Pathe PP, Biswas AK, Rao NN, Kaul SN (2005) Physico-chemical treatment of wastewater from clusters of small scale cotton textile units. Environ Technol 26(3):313–327

28. Bonyadi Z, Kumar PS, Foroutan R, Kafaei R, Arfaeinia H, Farjadfard S, Ramavandi B (2019) Ultrasonic-assisted synthesis of *Populus alba* activated carbon for water defluorination: application for real wastewater. Korean J Chem Eng 36(10):1595–1603

29. Zhang K, Cheung W, Valix M (2005) Roles of physical and chemical properties of activated carbon in the adsorption of lead ions. Chemosphere 60(8):1129–1140

30. Wilson K, Yang H, Seo CW, Marshall WE (2006) Select metal adsorption by activated carbon made from peanut shells. Bioresour Technol 97(18):2266–2270

31. Pandharipade S, Moharkar Y, Thakur R (2012) Synthesis of adsorbents from waste materials such as ziziphus jujube seed & mango kernel. Int J Eng Res Appl 2(4):2–5

32. Al-Othman ZA, Ali R, Naushad M (2012) Hexavalent chromium removal from aqueous medium by activated carbon prepared from peanut shell: adsorption kinetics, equilibrium and thermodynamic studies. Chem Eng J 184:238–247

33. Boehm HP (2002) Surface oxides on carbon and their analysis: a critical assessment. Carbon 40(2):145–149

34. Foroutan R, Mohammadi R, Razeghi J, Ramavandi B (2019) Performance of algal activated carbon/Fe3O4 magnetic composite for cationic dyes removal from aqueous solutions. Algal Res 40:101509

35. Guo Y, Rockstraw DA (2006) Physical and chemical properties of carbons synthesized from xylan, cellulose, and Kraft lignin by H3PO4 activation. Carbon 44(8):1464–1475

36. Bulut Y (2007) Removal of heavy metals from aqueous solution by sawdust adsorption. J Environ Sci 19(2):160–166

37. Reffas A, Bernardet V, David B, Reinert L, Lehocine MB, Dubois M, Batisse N, Duclaux L (2010) Carbons prepared from coffee grounds by H3PO4 activation: characterization and adsorption of methylene blue and Nylosan Red N-2RBL. J Hazard Mater 175(1–3):779–788

38. El-Hendawy A-NA (2009) The role of surface chemistry and solution pH on the removal of Pb2+ and Cd2+ ions via effective adsorbents from low-cost biomass. J Hazard Mater 167(1–3):260–267

39. Kazemipour M, Ansari M, Tajrobehkar S, Majdzadeh M, Kermani HR (2008) Removal of lead, cadmium, zinc, and copper from industrial wastewater by carbon developed from walnut, hazelnut, almond, pistachio shell, and apricot stone. J Hazard Mater 150(2):322–327

40. Sharma N, Kaur K, Kaur S (2009) Kinetic and equilibrium studies on the removal of Cd2+ ions from water using polyacrylamide grafted rice (*Oryza sativa*) husk and (*Tectona grandis*) saw dust. J Hazard Mater 163(2–3):1338–1344

41. Naeimi B, Foroutan R, Ahmadi B, Sadeghzadeh F, Ramavandi B (2018) Pb(II) and Cd(II) removal from aqueous solution, shipyard wastewater, and landfill leachate by modified *Rhizopus oryzae* biomass. Mater Res Express 5(4):045501

42. Foroutan R, Mohammadi R, Farjadfard S, Esmaeili H, Saberi M, Sahebi S, Dobaradaran S, Ramavandi B (2019) Characteristics and performance of Cd, Ni, and Pb bio-adsorption using *Callinectes sapidus* biomass: real wastewater treatment. Environ Sci Pollut Res 26(7):6336–6347

43. Foroutan R, Khoo FS, Ramavandi B, Abbasi S (2017) Heavy metals removal from synthetic and shipyard wastewater using *Phoenix dactylifera* activated carbon. Desalin Water Treat 82:146–156

44. Pyrzynska K (2019) Removal of cadmium from wastewaters with low-cost adsorbents. J Environ Chem Eng 7(1):102795

45. Luo M, Lin H, He Y, Li B, Dong Y, Wang L (2019) Efficient simultaneous removal of cadmium and arsenic in aqueous solution by titanium-modified ultrasonic biochar. Bioresour Technol 284:333–339

46. Zhang G, Fu P, Yang H, Fu P, Li Z (2019) Utilization of alkaline silicate wastes for removal of cadmium ions from aqueous solution: comparative performances and removal mechanisms. J Environ Chem Eng 7(5):103402

47. Naeem MA, Imran M, Amjad M, Abbas G, Tahir M, Murtaza B, Zakir A, Shahid M, Bulgariu L, Ahmad I (2019) Batch and column scale removal of cadmium from water using raw and acid activated wheat straw biochar. Water 11(7):1438

48. Chen R, Zhao X, Jiao J, Li Y, Wei M (2019) Surface-modified biochar with polydentate binding sites for the removal of cadmium. Int J Mol Sci 20(7):1775

49. Zheng L, Peng D, Meng P (2019) Corncob-supported aluminium-manganese binary oxide composite enhanced removal of cadmium ions. Colloids Surf A 561:109–119

50. Li M, Xiao X, Wang S, Zhang X, Li J, Pavlostathis SG, Luo X, Luo S, Zeng G (2020) Synergistic removal of cadmium and organic matter by a microalgae-endophyte symbiotic system (MESS): an approach to improve the application potential of plant-derived biosorbents. Environ Pollut 261:114177

51. Chen W, Lu Z, Xiao B, Gu P, Yao W, Xing J, Asiri AM, Alamry KA, Wang X, Wang S (2019) Enhanced removal of lead ions from aqueous solution by iron oxide nanomaterials with cobalt and nickel doping. J Clean Prod 211:1250–1258

52. Ahmad N, Sereshti H, Mousazadeh M, Rashidi Nodeh H, Kamboh MA, Mohamad S (2019) New magnetic silica-based hybrid organic-inorganic nanocomposite for the removal of lead(II) and nickel(II) ions from aqueous solutions. Mater Chem Phys 226:73–81

53. Li R, Deng H, Zhang X, Wang JJ, Awasthi MK, Wang Q, Xiao R, Zhou B, Du J, Zhang Z (2019) High-efficiency removal of Pb(II) and humate by a CeO2–MoS2 hybrid magnetic biochar. Bioresour Technol 273:335–340

54. Gu P, Zhang S, Zhang C, Wang X, Khan A, Wen T, Hu B, Alsaedi A, Hayat T, Wang X (2019) Two-dimensional MAX-derived titanate nanostructures for efficient removal of Pb(ii). Dalton Trans 48(6):2100–2107

55. Gupta S, Babu B (2009) Removal of toxic metal Cr (VI) from aqueous solutions using sawdust as adsorbent: equilibrium, kinetics and regeneration studies. Chem Eng J 150(2–3):352–365

56. Foroutan R, Ahmadlouydarab M, Ramavandi B, Mohammadi R (2018) Studying the physicochemical characteristics and metals adsorptive behavior of CMC-g-HAp/Fe3O4 nanobiocomposite. J Environ Chem Eng 6(5):6049–6058

57. Weber WJ, Morris JC (1963) Kinetics of adsorption on carbon from solution. J Sanit Eng Div 89(2):31–60

58. Kapur M, Mondal MK (2013) Mass transfer and related phenomena for Cr (VI) adsorption from aqueous solutions onto *Mangifera indica* sawdust. Chem Eng J 218:138–146

59. Ofomaja AE, Unuabonah EI (2013) Kinetics and time-dependent Langmuir modeling of 4-nitrophenol adsorption onto Mansonia sawdust. J Taiwan Inst Chem Eng 44(4):566–576

60. Njikam E, Schiewer S (2012) Optimization and kinetic modeling of cadmium desorption from citrus peels: a process for biosorbent regeneration. J Hazard Mater 213:242–248

61. Gupta V, Nayak A (2012) Cadmium removal and recovery from aqueous solutions by novel adsorbents prepared from orange peel and Fe2O3 nanoparticles. Chem Eng J 180:81–90